Electrochemical and Optical Properties of the Poly(3,4-ethylenedioxythiophene) Film Electropolymerized in an Aqueous Sodium Dodecyl Sulfate and Lithium Tetrafluoroborate Medium

Chun Li and Toyoko Imae*

Research Center for Materials Science, Nagoya University, Chikusa, Nagoya 464-8602, Japan

Received August 12, 2003; Revised Manuscript Received January 30, 2004

ABSTRACT: The poly(3,4-ethylenedioxythiophene) (PEDOT) films prepared in an aqueous sodium dodecyl sulfate and lithium tetrafluoroborate electrolyte solution were investigated. It was shown that the PEDOT films prepared in this medium exhibit novel electrochemical and optical properties. Cyclic voltammetric results indicate that the dodecyl sulfate (DS^-) anions are trapped in the polymer matrix when PEDOT is deposited onto the gold substrate. The larger DS^- anions are immobile and stay in the polymer during a redox process, whereas cation movement dominates the charge compensation, moving in and out of the polymer matrix, when the PEDOT film is redox-cycled. The infrared and X-ray photoelectron spectroscopic results further confirmed the incorporation of DS^- into the PEDOT film. Surface plasmon resonance was used to investigate the film growth and the optical properties of PEDOT films upon doping and dedoping at two laser wavelengths. With the film growing, an increase in doping level as well as an increase in refractive index was detected. The resonance curves change dramatically when the PEDOT film is switched to different doping states, suggesting important changes on the film dielectric constant and electrochromic property.

1. Introduction

Poly(3,4-ethylenedioxythiophene) (PEDOT), a highly conductive, stable, and transparent polythiophene derivative, has been widely investigated during the past decade due to its very remarkable properties and potential applications in many fields.[1−5] The PEDOT can be prepared using chemical oxidation polymerization or electrochemical polymerization of the monomer. Usually, the chemical polymerization results in a black, insoluble, infusible, and intractable compound, whereas electrode-supported and free-standing films of PEDOT can be obtained by electrochemical polymerization in both organic and aqueous media.[4] At the initial stage, the electropolymerization of 3,4-ethylenedioxythiophene (EDOT) was focused on the organic media,[6−12] due to its low solubility (2.1 mg cm^{-3} at 20 °C) in water and its higher oxidation potential than water, and the electropolymerization of thiophene precursors in aqueous media generally produces poorly defined materials. However, the aqueous medium stands out as it is more economic and environmentally attractive. As a solution to this problem, the use of anionic surfactants has been proposed by Sakmeche and co-workers,[13] which can increase the solubility of the monomer and decrease its oxidation potential, showing a distinct electrocatalytic effect. To date, the work concerning the electropolymerization of EDOT in aqueous media[13−16] is considerably less than that in organic media. Moreover, the structure and properties of PEDOT films prepared from aqueous media are still not well understood as well as the doping mechanism.

In the present paper, we report the electropolymerization of EDOT in an aqueous sodium dodecyl sulfate (SDS) and lithium tetrafluoroborate medium. It has been confirmed that the electrochemical and optical properties of the PEDOT films are, to a large extent, dependent on the condition of synthesis and especially the component of the electrolytes and the counterion incorporated as dopant during electropolymerization. The electrochemical and optical properties of the PEDOT films and their structure were investigated by cyclic voltammetry (CV), Fourier transform infrared (FT-IR) spectroscopy, X-ray photoelectron spectroscopy (XPS), ultraviolet−visible (UV−vis) spectroscopy, and surface plasmon resonance (SPR) spectroscopy.

2. Experimental Section

2.1. Materials. EDOT was purchased from Aldrich Chemical Co., lithium tetrafluoroborate ($LiBF_4$) was a product from Wako Pure Chemical Industries, Ltd., and SDS was obtained from Nakarai Chemicals Ltd. All chemicals were used as received without further purification. The aqueous solutions were prepared with ultrapure water (18.3 MΩ), which was prepared using a Milli-Q filtration unit from the Millipore Corp.

2.2. Electrochemistry. Voltammetric and potentiostatic experiments were performed in a one-compartment, three-electrode electrochemical cell with the use of a Hokuto-Denko model HZ-3000 automatic polarization system. The working electrode was an Au disk (2 mm diameter), and a Pt wire was used as counter electrode. All potentials were referred to a saturated calomel electrode (SCE). The electrolyte was an aqueous 0.07 M SDS and 0.1 M $LiBF_4$ solution containing 0.03 M EDOT. All solutions were deoxygenated by nitrogen before the electrochemical measurements.

2.3. Fourier Transform Infrared Spectroscopy. FT-IR spectra were recorded at room temperature on a Bio-Rad FTS 575C FT-IR spectrometer equipped with a cryogenic mercury cadmium telluride (MCT) detector. The infrared reflectance absorption (IRA) spectrum was measured using a Harrick reflectance attachment with an incidence angle of 75°. A 200 nm thick Au film evaporated on glass substrate with a 150 nm chromium film as an adhesion layer were used as working electrode to deposit a PEDOT film for the IRA spectral measurement. The EDOT monomer spectrum was measured using transmission mode, in which a thin layer of the liquid

* Corresponding author: Fax + 81-52-789-5912; Tel + 81-52-789-5911; e-mail imae@nano.chem.nagoya-u.ac.jp.

10.1021/ma035188w CCC: $27.50
Published on Web 03/05/2004

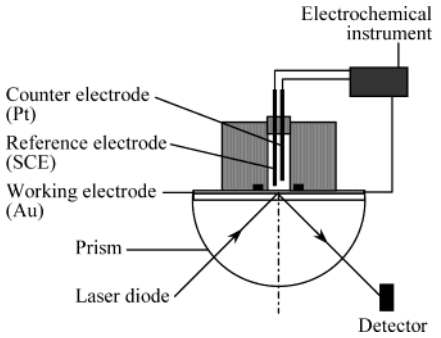

Figure 1. Schematic drawing of the experimental setup for in situ electrochemical SPR measurement.

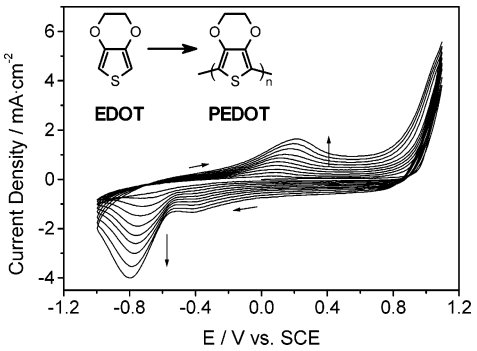

Figure 2. Cyclic voltammograms of 0.03 M EDOT in an aqueous solution of 0.07 M SDS and 0.1 M $LiBF_4$ on a gold electrode at a potential scan rate of 100 mV s^{-1}. Inset: chemical structures of EDOT and PEDOT. The cyclic scan was started from 0 V toward the anodic side. The sweep direction was added by arrows.

was spread between two KBr pellets. All spectra were collected for 256 interferograms at a resolution of 4 cm^{-1}. The PEDOT film for IRA measurement was prepared chronoamperostatically at 0.84 V vs SCE (q = 100 mC cm^{-2}).

2.4. X-ray Photoelectron Spectroscopy. XPS was performed at room temperature with an ESCA-3300 electron spectrometer (32 eV pass energy) equipped with a monochromatized Mg Kα (1253.6 eV) X-ray source operated at a power of 10.0 kV and a current of 30.0 mA. Pressure in the analysis chamber was lower than 2×10^{-7} Pa. The samples used for this analysis were the films prepared chronoamperostatically at 0.84 V vs SCE (q = 200 mC cm^{-2}). The doped PEDOT film is the as-grown one at 0.84 V vs SCE, whereas the dedoped PEDOT film was prepared by holding the film at the potential of −1.0 V for 10 min in a monomer-free electrolyte solution. To thoroughly remove the adsorbed SDS and monomer on the film, the films were soaked in water for 1 h, followed by copious rinsing with water and acetone, and then dried overnight at room temperature in vacuo before characterization.

2.5. In Situ Ultraviolet−Visible Spectroscopy. The in situ UV−vis spectra were recorded at room temperature on a Shimadzu UV-2200 spectrometer with a simple quartz cuvette (10 mm path length) as the electrochemical cell. A thin PEDOT film was deposited chronamperostatically onto ITO-coated glass (0.84 V vs. SCE, q = 13 mC cm^{-2}) with the same counter and reference electrodes in the electrolyte system described above.

2.6. Electrochemical Surface Plasmon Resonance Setup. The schematic illustration of the setup for the excitation of surface plasmons in the Kretschmann optical configuration combined with an electrochemical cell is shown in Figure 1. An Au film on a glass slide (Nippon Laser & Electronics Lab.) was used as both a working electrode (0.07 cm^2 for electrolyte contact) and the SPR substrate. The counter electrode was a platinum wire, and a SCE was used as reference. All SPR spectra were recorded at 30 °C with a Biosensor Analytical System (Nippon Laser & Electronics Lab). The linearly p-polarized light (λ = 670 and 780 nm) from a laser diode was used to investigate the films. The reflected signal beam from the sample surface was measured by a photodiode detector. The growth process of the PEDOT film was monitored by SPR measurements, recording the SPR angular scan curves at the oxidized and reduced states. A deoxygenated aqueous 0.1 M $LiBF_4$ and 0.07 M SDS solution containing 0.03 M EDOT was filled in the cell, and the PEDOT film was deposited by cycling the potential between −1.0 and 0.85 V on an Au glass slide. After the given cycles were scanned, the potential was set at 0.65 and −1.0 V to measure the angular scan curves. The electrochromic process of the PEDOT film on a gold chip was detected by angular measurement, which was performed by scanning an incident angle range while holding the potential of the working electrode at the given value.

3. Results and Discussion

3.1. Electropolymerization of EDOT and Electrochemical Properties of the PEDOT Film. The successive cyclic voltammograms of 0.03 M EDOT on an Au electrode in an aqueous medium (0.07 M SDS + 0.1 M $LiBF_4$) by potential scanning between −1.0 and 1.1 V vs SCE are shown in Figure 2. It is clear from the first voltammetric curve that a rapid growth of the anodic current density starts around 0.76 V, which corresponds to the beginning of the EDOT monomer oxidation. This value is much lower than that observed in an organic medium (1.10 V vs SCE in a 0.1 M $LiClO_4$ acetonitrile solution).[9] This distinct decrease (0.34 V) of the oxidation potential in an aqueous medium with respect to that in acetonitrile can be attributed to the specific effect of the anionic surfactant.[15] During the successive potential scans, the PEDOT film was deposited on the electrode surface. The polymer was reduced and oxidized between −0.8 and 0.2 V, which will be discussed later more in detail. The increase of the anodic and cathodic peak current densities increased, implying that the amount of the polymer on the electrode surface increased.

To find optimum conditions for the PEDOT film deposition, the electrochemical polymerization of EDOT was conducted in the potentiostatic mode at different potentials. The potential was first switched from open-circuit potential to 0.5 V for 100 s before polarizing the electrode to the desired potential. This initial step was to allow double-layer charging of the Au electrode|solution interface, which minimizes the distortion of the polymerization current transient by double-layer capacitance charging.[17,18] The chronoamperometric curves recorded between 0.76 and 0.88 V are shown in Figure 3. The electropolymerization in the potentiostatic mode includes three successive steps: nucleation, corresponding to the creation of the first active centers; polymer growth on the electrode; and diffusion of the electroactive species within the deposited film.[8,15,17,18] An optimal potential value exists for which the current density remains constant during all the electrolysis time after the nucleation, which corresponds to the formation of a conductive polymer film. Moreover, usually the decrease of the monomer concentration and polarization potential favors the formation of a compact and smooth film on the electrode surface. A uniform and smooth film is required for the structure characterization and the property measurements. On the basis of this knowledge and the chronoamperometric curves (Figure 3), relatively low potentials (0.82−0.84 V vs SCE) and a monomer concentration (0.03 M) were chosen for the preparation of PEDOT films for the characterization.

Chart 1

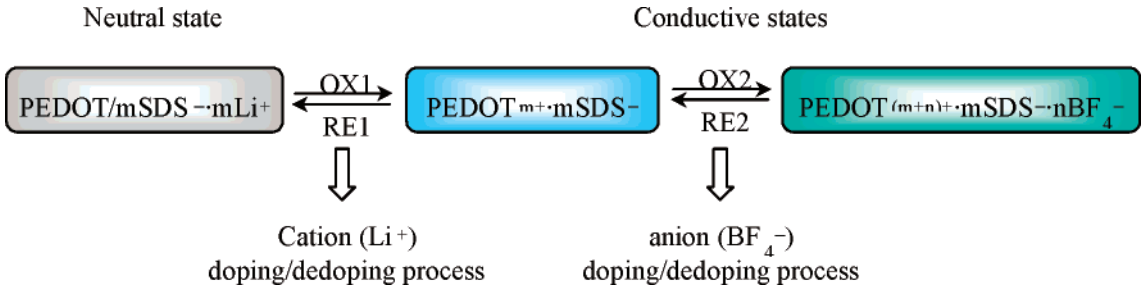

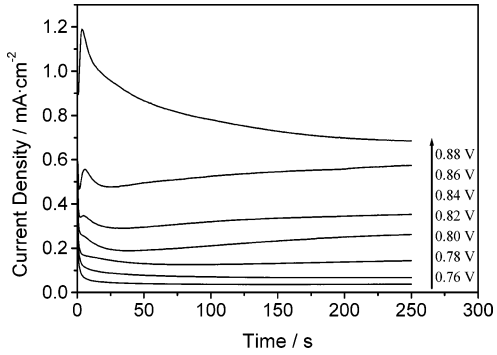

Figure 3. Chronoamperograms of 0.03 M EDOT in an aqueous solution of 0.07 M SDS and 0.1 M $LiBF_4$ on a gold electrode at the given potentials.

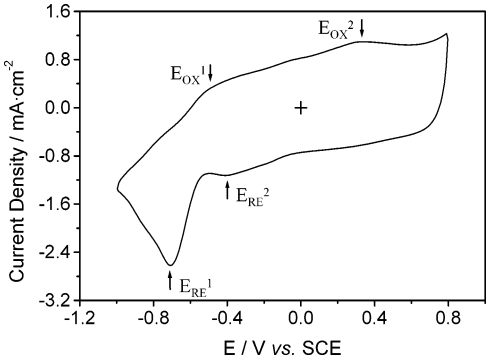

Figure 4. Cyclic voltammogram of the PEDOT film deposited on a gold electrode in an aqueous solution of 0.1 M $LiBF_4$ at a potential scan rate of 100 mV s^{-1}.

Figure 4 shows a cyclic voltammogram of the PEDOT film (which was prepared by successive potential scanning through seven cycles from −1.0 to 1.1 V in the electrolyte described above) on an Au electrode in an aqueous 0.1 M $LiBF_4$ solution without SDS. Two sets of redox peaks were observed. The first oxidation peak is located around −0.5 V, and the corresponding reduction peak at −0.7 V is very strong and narrow; the second anodic peak was found at 0.33 V, and the reduction peak is around −0.4 V. This redox behavior is quite different from those of PEDOT films reported previously.[7,11,15] The existence of these two sets of redox peaks indicates that a dual mode of ion exchange (both anion and cation exchanges) is involved in the redox process for the PEDOT film (Chart 1), which is the same as polypyrrole/surfactant films.[19,20] The first oxidation peak (E_{ox}^1) is due to the movement of cations out of the polymer, and the second oxidation peak (E_{ox}^2) is ascribed to anion movement taking over when the number of charges on the polymer exceeds the number of bound DS^- anions remaining in the polymer. Under the existence of the larger dopant ion (DS^-), cation movement becomes dominating compared to anion movement

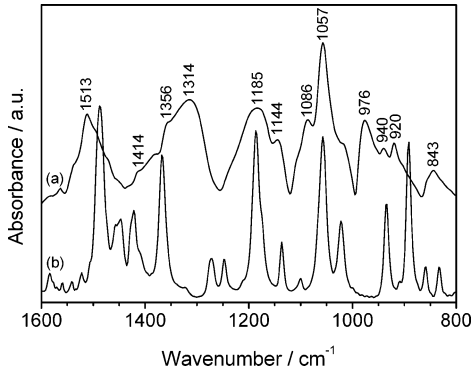

Figure 5. Infrared reflectance absorption spectrum of the undoped PEDOT film (a) and a transmission FTIR spectrum of the EDOT monomer (b) in the 1600−800 cm^{-1} region.

because the larger dopant anions are more strongly bound to the polymer and thus have less tendency to be replaced by smaller, mobile BF_4^- anions. During potential scanning to more negative values, the creation of the open, water-swelled structure of the polymer in the reduced state is a cooperative process involving the simultaneous participation of several polymer segments. Because of the stabilization, the reduction potential is shifted to more negative values, and the cooperative nature causes the reaction to occur over a narrow potential range, which is similar to the polypyrrole/surfactant films reported in the literature[20] but different from the PEDOT film prepared in an organic system with small dopants.[7] An additional reduction peak around −0.4 V is due to the movement of BF_4^- anions out of the polymer films.

3.2. FT-IR and XPS Spectra and the Components of the PEDOT Film. Figure 5 shows the FTIR spectrum of the dedoped PEDOT film together with the monomer spectrum. It is clear that the strong band ascribed to the C−H bending mode at 891 cm^{-1} disappears in the polymer spectrum in comparison with the monomer spectrum, demonstrating the formation of PEDOT chains with α,α′-coupling. Vibrations at 1513, 1414, and 1356 cm^{-1} are attributed to the stretching modes of C═C and C−C in the thiophene ring.[9,10] The vibration modes from the C−S bond in the thiophene ring[9] can be seen at 940 and 843 cm^{-1}. The bands at 1144 and 1057 cm^{-1} are assigned to the stretching modes of the ethylenedioxy group, and the band around 920 cm^{-1} is due to the ethylenedioxy ring deformation mode.[9,10] It is worthwhile to note that the strong bands located around 1314, 1185, 1086, and 976 cm^{-1}, attributable to the stretching vibrations of the sulfate group,[21] can be clearly seen, which should be from the DS^- anions incorporated into the polymer matrix. These bands change little when switching the film from the oxidized to reduced state, suggesting that the DS^- anions remain trapped in the film.

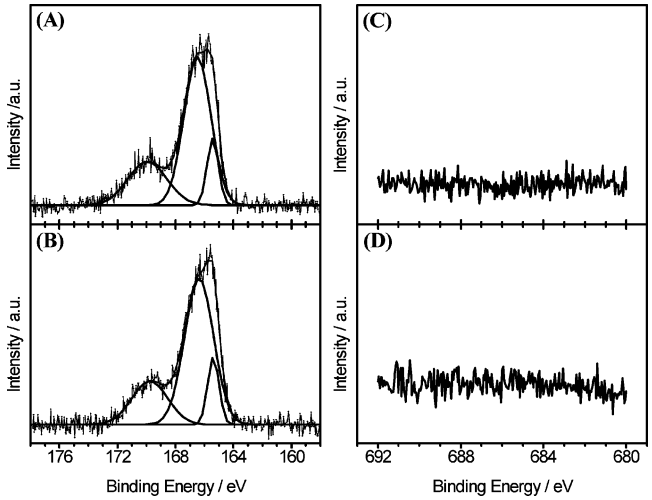

Figure 6. High-resolution XPS spectra for PEDOT films. The S_{2p} region: (A) oxidized film (as-grown at 0.84 V); (B) reduced film (−1.0 V). The F_{1s} region: (C) oxidized film (as-grown at 0.84 V); (D) reduced film (−1.0 V).

To further confirm the incorporation of DS^- anions in the films and evaluate the doping level, the PEDOT films (0.82 V vs. SCE, $q = 200$ mC cm^{-2}) in the oxidized and reduced states were analyzed by XPS. The constituent elements of the PEDOT films, carbon, oxygen, and sulfur, are clearly detected from the general XPS spectra (not shown here) in both states. Figure 6 displays the high-resolution spectra recorded for oxidized and reduced PEDOT films. The S_{2p} spectral regions have been further analyzed by the peak deconvolution. The S_{2p} signals for PEDOT films include two components. The first one can be deconvoluted into two peaks, 166.43 and 165.40 eV, respectively, attributable to the thiophene sulfur atom. The second component located at 169.85 eV is ascribed to the sulfur atom of the DS^- anions, remaining trapped in the film. However, neither oxidized nor reduced films have an affinity for BF_4^-, as confirmed by the absence of peaks in the fluorine region (F_{1s}) (Figure 6C,D). This result seems contradictory with the conclusion obtained by the cyclic voltammetric measurement, i.e., the BF_4^- anion is involved in the redox process of PEDOT film, and the F_{1s} signal should be detected in the oxidized film. This difference may be caused by the posttreatment of the PEDOT film for XPS measurements because the BF_4^- anion has been completely removed by washing, since the interaction between DS^- and the charges on the one-dimensional polymer chains is much stronger than that between BF_4^- and charged polymer chain.

The doping level of DS^- anion in the PEDOT film calculated from the atomic ratio is about 0.36, which is a little bit higher than the value (0.3) reported in the literature for polythiophene and its derivatives.[8] The excess part from the value in the literature is most likely undissociated sodium dodecyl sulfate, since the tendency for incorporation of neutral molecules in the polymer is expected to increase when the hydrophobic fraction of the polymer increases. A similar result has been observed for polypyrrole film doped with larger alkyl benzenesulfonates.[19,20]

3.3. In-Situ UV−vis Spectra and the Electronic Structure of the PEDOT Film. In situ UV−vis spectra were recorded, while a PEDOT film ($q = 13$ mC cm^{-2}) was kept at potentials between −0.8 and 0.65 V in a monomer-free electrolyte solution. The potential-dependent spectra are shown in Figure 7. It is clear that the dedoped PEDOT film (−0.8 V vs SCE) exhibits a wide absorption band centered at 600 nm, ascribed to the $\pi-\pi^*$ electronic transition.[9−11,15] Upon oxidation, the intensity of this band decreases and the absorbance at the longer-wavelength region increases gradually, as reported previously for the PEDOT film synthesized in organic and aqueous media.[9−11,15] Then, the film in the oxidized state can be considered as practically transparent in the visible range. It is noted from UV−vis spectra in Figure 7 that an isosbestic point exists around 720 nm, when the potential is less than 0 V, and there is an opposite change in the absorbance on different sides of the isosbestic point. Therefore, in this work two laser wavelengths (λ = 670 and 780 nm) were used to investigate the SPR response at different states in the next section.

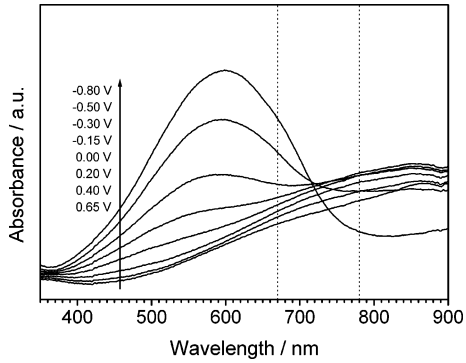

Figure 7. In-situ UV−vis absorption spectra of the PEDOT film at different potentials on an ITO electrode in a monomer-free electrolyte solution.

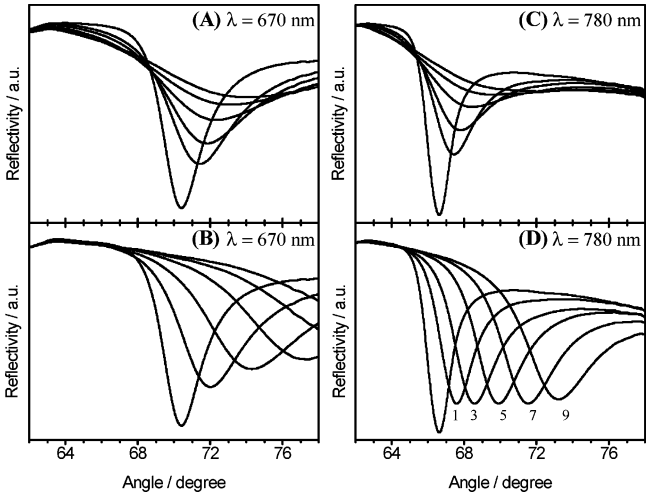

Figure 8. SPR angular scan curves recorded at oxidized (0.65 V: A, C) and reduced (−1.0 V: B, D) states of the PEDOT films after 1, 3, 5, 7, and 9 potential cycles between −1.0 and 0.85 V under different laser wavelengths. The leftmost curve in each figure is the SPR curve of the bare gold electrode in pure water.

3.4. SPR Spectra and Conductivity of the PEDOT Film. SPR has been shown to be a powerful tool with high sensitivity for studying ultrathin films.[22,23] Recently, the combination of SPR with electrochemical techniques for the characterization of ultrathin conducting polymer films has been demonstrated.[12,24−27] Figure 8 presents the SPR angular scan curves recorded for the oxidized (0.65 V; A, C) and reduced (−1.0 V; B, D) states of PEDOT films prepared by 1, 3, 5, 7, and 9 potential scans between −1.0 and 0.85 V in an electro-

lyte solution described in the Experimental Section at two different laser wavelengths (λ = 670 and 780 nm). The leftmost curve in each figure is the SPR spectrum of bare gold chip in pure water. It is clear that in both oxidized and reduced states, with increasing cycles, the SPR resonance curve shows a shift to higher angles relative to that of the bare gold chip, and simultaneously the dip intensity and width also show a distinct change.

Usually the shift in the resonance angle can readily be associated with a change in refractive index and an increase in the film thickness, whereas the change in shape of the reflectance curve is characteristic of a change in the imaginary part of the complex dielectric constant, i.e., the extinction coefficient, which can be measured by the absorption spectra.[24,25] It is well-known that, for conducting polymers, the optical constants are related to film conductivity. For incident light with a wavelength λ impinging on a material with conductivity σ, the complex dielectric constant can be expressed as[24]

$$\epsilon = \epsilon_{\text{real}} + i(2\sigma\lambda/c)$$

where c is the velocity of light. The imaginary part of the dielectric constant, $\epsilon_{\text{imag}} = 2\sigma\lambda/c$, is related to the optical absorption of the film. It is clear that the variation of the film conductivity can cause a large change in the imaginary part of the dielectric constant. Therefore, the redox transition leads to a large change in shape of the SPR curves. We find from Figure 8 that the shape change becomes more distinct for a thicker PEDOT film and depends on the laser wavelength.

Recently, Shi and co-workers[28] have reported that conducting polymers such as polypyrrole, poly(*p*-phenylene), and polythiophene were formed almost in a neutral state initially, and then the doping degrees increased gradually up to constant values with increasing thickness, which make the imaginary part of the dielectric constant increase. Therefore, during continuous potential cycling in the present work, the increase in doping level as well as the increase in refractive index accompanies the increase of the PEDOT film thickness, resulting in the increase of the dip intensity and the distinct enlargement of the dip width. It is worth noting here that the dip intensity in Figure 8D shows a slight dependence on the thickness of the PEDOT film, and the width of the resonance dip exhibits a small enlargement. This characteristic corresponds to the smallest absorption (smaller ϵ_{imag} value) of the reduced PEDOT film at 780 nm compared with the other three states.

3.5. SPR Spectra of the PEDOT Film at Different Doping States and Its Novel Optical Properties. Figure 9 shows potential-dependent SPR curves of a thin PEDOT film that was polymerized potentiostatically on an Au chip (0.82 V vs SCE, q = 3.7 mC cm^{-2}) at two different laser wavelengths. The reflectivity measurements were carried out under equilibrium conditions where the potentials were held constant. It can be seen from this figure that significant changes, including resonance angle, dip intensity, and dip width, are induced during the doping and dedoping processes. For both laser wavelengths, the resonance angles of the dips shift to larger values upon reducing the film from oxidized state to neutral state. Simultaneously, for λ = 670 nm, the curves became broader, and the dip intensity increases, while the resonance dip at 780 nm deepened and became narrower. To further analyze these results, one needs to recall the description above that the SPR signal is really sensitive to changes in the

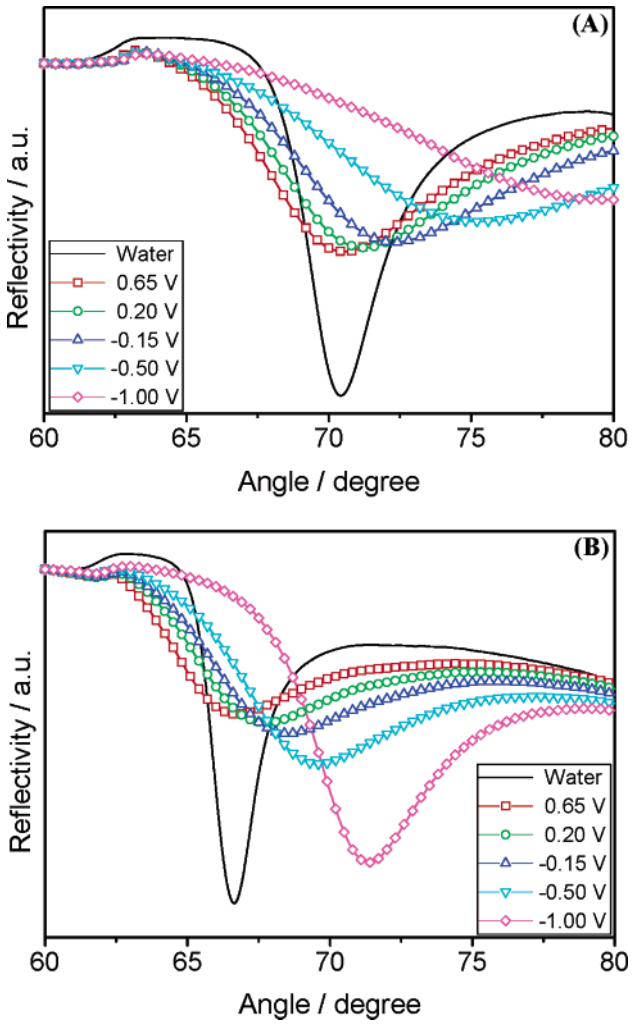

Figure 9. SPR angular scan curves of a thin PEDOT film (0.82 V vs SCE, q = 3.7 mC cm^{-2}) on a gold chip under different potentials at two different wavelengths: (A) 670 nm and (B) 780 nm.

film complex dielectric constant, thickness, and film structure. It is well-known that, for a conducting polymer, cycling of the film between the oxidized and the reduced states is accompanied by volume changes. The film expands upon doping of a small anion as dopant and contracts upon dedoping. However, in the present work, the PEDOT film doped by larger DS$^-$ anions has a charge-compensating scheme dominated by cation movement, which makes the film swell upon reduction and shrink upon oxidation, as Bag et al.[20] demonstrated. When the polymer is reduced from its oxidized state, the increase in the real part of the dielectric constant and the volume enlargement shift the resonance to a higher angle. At the same time, the imaginary part ($i\epsilon_{\text{imag}}$) also changes. Since the imaginary part of the dielectric constant is related to the extinction coefficient at a given wavelength, opposite SPR behavior was observed at λ = 670 nm and λ = 780 nm, corresponding to the opposite behavior of absorbance at each side of the isosbestic point. At λ = 670 nm, the imaginary part of the dielectric constant increases upon dedoping of the polymer, which make the dip intensity increase and the width of resonance dip enlarge, whereas at λ = 780 nm, there are opposite changes in these values. This novel electrochromic phenomenon of the PEDOT film observed by SPR in aqueous solutions

suggests the potential application of PEDOT in biosensors.[5,27,29]

4. Conclusions

The structure and properties of poly(3,4-ethylenedioxythiophene) films doped with dodecyl sulfate were investigated by electrochemical and various spectroscopic techniques. It has been demonstrated that large dodecyl sulfate anions are immobile and stay in the polymer matrix during redox processes and that cation movement dominates the charge compensation, exhibiting novel redox properties. The combination of electrochemistry and surface plasmon resonance methods was used to monitor the growth process of the PEDOT film. The novel electrochromic behavior of PEDOT film observed by SPR in aqueous solutions suggests the potential application of PEDOT in biosensors.

References and Notes

(1) Granström, M.; Berggren, M.; Inganäs, O. *Science* **1995**, *267*, 1497.
(2) McCullough, R. D. *Adv. Mater.* **1998**, *10*, 93.
(3) Bobacka, J. *Anal. Chem.* **1999**, *71*, 4932.
(4) Groenendaal, L.; Jonas, F.; Freitag, D.; Pielartzik, H.; Reynolds, J. *Adv. Mater.* **2000**, *12*, 481 and references therein.
(5) Kros, A.; van Hövell, S. W. F. M.; Sommerdijk, N. A. J. M.; Nolte, R. J. M. *Adv. Mater.* **2001**, *13*, 1555.
(6) Pei, Q.; Zuccarello, G.; Ahlskog, M.; Inganäs, O. *Polymer* **1994**, *35*, 1347.
(7) Chen, X.; Inganäs, O. *J. Phys. Chem.* **1996**, *100*, 15202.
(8) Randriamahazaka, H.; Nol, V.; Chevrot, C. *J. Electroanal. Chem.* **1999**, *472*, 103.
(9) Kvarnström, C.; Neugebauer, H.; Blomquist, S.; Ahonen, H. J.; Kankare, J.; Ivaska, A. *Electrochim. Acta* **1999**, *44*, 2739.
(10) Garreau, S.; Louarn, G.; Buisson, J. P.; Froyer, G.; Lefrant, S. *Macromolecules* **1999**, *32*, 6807.
(11) Ahonen, H. J.; Lukkari, J.; Kankare, J. *Macromolecules* **2000**, *33*, 6787.
(12) Xia, C.; Advincula, R. C.; Baba, A.; Knoll, W. *Langmuir* **2002**, *18*, 3555.
(13) Sakmeche, N.; Aaron, J.-J.; Fall, M.; Aeiyach, S.; Jouini, M.; Lacroix, J. C.; Lacaze, P.-C. *Chem. Commun.* **1996**, 2723.
(14) Lima, A.; Schottland, P.; Sadki, S.; Chevrot, C. *Synth. Met.* **1998**, *93*, 33.
(15) Sakmeche, N.; Aeiyach, S.; Aaron, J.-J.; Jouini, M.; Lacroix, J. C.; Lacaze, P.-C. *Langmuir* **1999**, *15*, 2566.
(16) Garreau, S.; Duvail, J. L.; Louarn, G. *Synth. Met.* **2002**, *125*, 325.
(17) Hillman, A. R.; Mallen, E. F. *J. Electroanal. Chem.* **1987**, *220*, 351.
(18) Li, F.; Albery, W. J. *Electrochim. Acta* **1992**, *37*, 393.
(19) Naoi, K.; Oura, Y.; Maeda, M.; Nakamura, S. *J. Electrochem. Soc.* **1995**, *142*, 417.
(20) Bay, L.; Mogensen, N.; Skaarup, S.; Sommer-Larsen, P.; Jørgensen, M.; West, K. *Macromolecules* **2002**, *35*, 9345.
(21) Barr, G. E.; Sayre, C. N.; Connor, D. M.; Collard, D. M. *Langmuir* **1996**, *12*, 1395.
(22) Knoll, W. *Annu. Rev. Phys. Chem.* **1998**, *49*, 569 and references therein.
(23) Imae, T. In *Encyclopedia of Surface and Colloid Science*; Marcel Dekker: New York, 2002, 3547.
(24) Georgiadis, R.; Peterlinz, K. A.; Rahn, J. R.; Peterson, A. W.; Grassi, J. H. *Langmuir* **2000**, *16*, 6759.
(25) Xiao, X.; Jin, Y.; Cheng, G.; Dong, S. *Langmuir* **2002**, *18*, 1713.
(26) Baba, A.; Advincula, R. C.; Knoll, W. *J. Phys. Chem. B* **2002**, *106*, 1581.
(27) Raitman, O. A.; Katz, E.; Bückmann, A. F.; Willmer, I. *J. Am. Chem. Soc.* **2002**, *124*, 6487.
(28) Shi, G.; Xu, J.; Fu, M. *J. Phys. Chem. B* **2002**, *106*, 288.
(29) Constantine, C. A.; Mello, S. V.; Dupont, A.; Cao, X.; Santos, D., Jr.; Oliveira, O. N., Jr.; Strixino, F. T.; Pereira, E. C.; Cheng, T.-C.; Defrank, J. J.; Leblanc, R. M. *J. Am. Chem. Soc.* **2003**, *125*, 1805.

MA035188W